ACS OMEGA

Article

Cite This: ACS Omega 2018, 3, 17359−17367

http://pubs.acs.org/journal/acsodf

Fabrication of Biodegradable Poly(naringin) Particles with Antioxidant Activity and Low Toxicity

Mehtap Sahiner,[†,∥] Nurettin Sahiner,*[,‡,§] Selin Sagbas,[‡] Mitchell L. Fullerton,[∥] and Diane A. Blake*[,∥]

[†]Fashion Design, Canakkale Applied Science and [‡]Nanoscience and Technology Research and Application Center (NANORAC), Faculty of Science and Arts, Department of Chemistry, Canakkale Onsekiz Mart University, Terzioglu Campus, 17100 Canakkale, Turkey

[§]Department of Physics & Engineering Physics, Tulane University, New Orleans, Louisiana 70118, United States

[∥]Department of Biochemistry and Molecular Biology, School of Medicine, Tulane University, New Orleans, Louisiana 70448, United States

Supporting Information

ABSTRACT: Naringin (NR, 4′,5,7 trihydrocyflavanone-7-*O*-rhamnoglucoside) is a flavanone found in citrus fruit that is composed of a phenolic compound, naringenin, and a disaccharide, neohesperidose. Poly(NR) [p(NR)] particles in the size range of few micrometers to few hundred nanometers were prepared from highly purified NR and subsequently characterized using UV/visible spectroscopy, Fourier transform infrared spectroscopy, nuclear magnetic resonance spectroscopy, scanning electron microscopy, thermogravimetric analysis, and zeta potential measurements. The hydrolytic degradation of p(NR) particles at 37.5 °C was investigated at pHs 5.4, 7.4, and 9.0. The particles degraded most rapidly at pH 7.4, with >90% degradation after 5 h. The cytotoxicity was assessed by growing COS-1 fibroblasts for 5 days in the presence of increasing concentrations of NR or eluates from the p(NR) particles. Both NR and p(NR) particles were nontoxic for these mammalian fibroblasts; at the highest concentration tested (571 μg/mL), the percentages of surviving cells after 5 days in culture were 96.7 ± 0.93 and 91 ± 11% for NR and p(NR), respectively. The effect of p(NR) on red blood cell hemolysis was also negligible (<2%) at concentrations up to 100 μg/mL; unpolymerized NR showed slightly higher levels of hemolysis than the p(NR) particles, but values never exceeded 5% at 50 and 100 μg/mL. Both NR and p(NR) stimulated blood coagulation in a dose-dependent manner; the hemostatic effect was greater for p(NR), which, at 100 μg/mL, stimulated in vitro blood clotting by ∼50%. Neither NR nor eluates from p(NR) particles inhibited α-glucosidase activity; in fact, both provided a modest (10−30%) stimulation at concentrations from 0.67 to 1.67 mg/mL. p(NR) particles are easily synthesized, break down readily at physiological pH, and have excellent blood and biocompatibility. As such, they will be a useful carrier for drug delivery and as an oral antioxidant supplement.

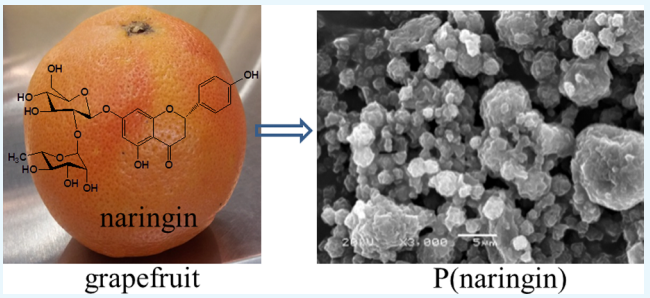

INTRODUCTION

In recent years, phenolic compounds have attracted attention because of their inherit antioxidant, antimicrobial, nontoxic, and natural characteristics. Plants and citrus fruits contain a wide variety of different phenolic compounds including, but not limited to limonene, naringin (NR), naringenin, hesperetin, neohesperidin, poncirin, and neoeriocitrin. Citrus flavanones also exist in both glycoside or aglycone forms.[1] NR is the form of naringenin that is substituted with a disaccharide composed of glucose and rhamnose. The sugars stabilize the aglycone, increase water solubility, and enhance bioavailability and biocompatibility.[2] As a flavone glycoside, NR is the predominant bitter component in grapefruit. In citrus juice industries, methods for eliminating NR, either by transformation to the flavorless aglycone or by selective absorption, are in demand to decrease the bitter taste of citrus juice.[3] However, this compound also has many health benefits, including antioxidant, anti-inflammatory, and anti-apoptotic properties.[3,4] Other reported biomedical benefits included: lowering of cholesterol via inhibition of HMG-CoA reductase; relieving neurodegenerative disorders; improving patients with diabetes mellitus; reducing osteoporosis and hypertension; and ameliorating rheumatological disorders.[4] The compound has also been reported to have anticancer, hepatoprotective, antimutagenic, and redox protective effects.[5−7] NR has low water solubility, lipophilicity, and a bitter taste.[8] These properties limit the quantities of NR that can be taken by oral ingestion, which is one of the main restrictive factors for

Received: September 5, 2018
Accepted: November 29, 2018
Published: December 14, 2018

DOI: 10.1021/acsomega.8b02292
ACS Omega 2018, 3, 17359−17367

its use as an oral supplement. NR can be extracted from citrus fruit and exists in relative high levels in grapefruit. In general, flavonoids have weak stability against the diverse environment stresses (heat, light, and oxidation).[8−15] In the literature, carriers that increase the stability and bioavailability of NR, including metal nanoparticles and metal−organic frameworks, have increased consumer acceptance.[16,17] Although NR is one of the primary flavonoids in grapefruit juice, it is not the component that enhances the oral bioavailability of commonly prescribed drugs, including statins, calcium channel blockers, and sildenafil (Viagra).[18] However, depending upon the administered dose, NR can inhibit other transporters on intestinal epithelial cells and may influence absorption of other drug classes.[19−21] Thus, methods to deliver NR orally without the adverse effects from other components of grapefruit juice could increase its use both as a natural antioxidant/anti-inflammatory dietary supplement and a drug delivery vehicle.

In this study, NR particles were synthesized via a microemulsion method using highly purified NR with trimethylolpropane triglycidyl ether (TMPGDE) as a cross-linker. The NR monomer and the corresponding particles were characterized via Fourier transform infrared (FT-IR) spectroscopy, nuclear magnetic resonance (NMR), high-performance liquid chromatography (HPLC), thermogravimetric analysis (TGA), and scanning electron microscopy (SEM) imaging. Antioxidant activities and biocompatibility of these particles were studied using tests that measured phenol content, free-radical scavenging activity, cytotoxicity, blood compatibility, and inhibition of the digestive enzyme, α-glucosidase. These studies demonstrate that poly(NR) [p(NR)] has excellent blood and biocompatibility and could be a natural, nontoxic carrier for use in biomedical applications.

EXPERIMENTAL SECTION

Materials. The following reagents were used as received: NR (≥95%, HPLC, Sigma), TMPGDE (technical grade, Aldrich) as a cross-linker, triethylamine (TEA, 99.5%, Sigma-Aldrich) as an accelerator, Span 80 (viscosity 1200−2000 mPa s—20 °C, Fluka) and L-α-lecithin (granular, 98%, Acros Organic) as surfactants, and cyclohexane (ACS reagent, 99.5%, Sigma-Aldrich), gasoline (95 octane, local vender), acetone (99%, BRK), and ethanol (99%, Birkim) as solvents. Folin−Ciocalteau's (FC) phenol reagent (Sigma-Aldrich) and 2,2′-azino-bis-(3-ethylbenzothiazoline-6-sulfonic acid) (ABTS, Aldrich) were used for antioxidant studies. All aqueous solutions were freshly prepared using ultrapure distilled water, 18.2 MΩ cm (Millipore-Direct-Q UV3).

Biocompatibility Tests. Neutral buffered formalin and toluidine blue were from Sigma-Aldrich Chemicals (St Louis, MO). Costar tissue culture plates (24-well) were obtained from Fisher Scientific. COS-1 cells (African monkey fibroblasts) were obtained from the American Type Culture Collection [(ATTC), Manassas, VA] and maintained as described by the ATCC. Fetal bovine serum (FBS) was purchased from Atlanta Biologicals (Lawrenceville, GA). Dulbecco's modified Eagle's medium (DMEM), L-glutamine, sodium pyruvate, and antibiotic−antimycotic (AA) solution (100×, containing penicillin, streptomycin, and amphotericin B) were from Life Technologies (Grand Island, NY). All reagents were used as received, without further purification.

Antioxidant Testing. Folin and Ciocalteu's phenol reagent, potassium persulfate, gallic acid, trolox (6-hydroxy-2,5,7,8-tetramethylchromane-2-carboxylic acid), ABTS, and diammonium salt were purchased from Sigma-Aldrich.

α-Glucosidase Activity. α-Glucosidase from *Saccharomyces cerevisiae* and *p*-nitrophenyl-α-D-glucopyranoside were obtained from Sigma-Aldrich. Buffers were prepared using reagent grade chemicals.

Synthesis of NR Particles. p(NR) particles were synthesized via a microemulsion cross-linking method in the lecithin/gasoline solution. NR solution was prepared by dissolution of 1 g of NR in 10 mL of 0.5 M NaOH solution. Then, 1 mL of NR solution was placed into 30 mL of 0.1 M lecithin in gasoline and stirred at 1000 rpm for 1 h. TEA (10 μL) and TMPGDE (89 μL, 200 mol % of NR) were added to this solution under constant mixing. After 4 h of reaction at room temperature, the particles were washed sequentially by suspension in 15 mL of the indicated solvents and subsequent centrifugation at 10 000 rpm: gasoline (1×), ethanol (3×), 50:50 ethanol/water (3×), and acetone (1×). Finally, the obtained particles were dried in an oven at 50 °C and stored in closed containers for further use.

Characterization of Particles. Optical (BX54, Olympus) and SEM (Jeol JSM-5600 LV) were employed to assess the shape, size, and surface structure of the particles.

For SEM, the particles were secured on a carbon tape and coated with gold to a few nanometers thickness in vacuum. Imaging was performed using an operating voltage of 20 kV. The particle sizes were also assessed using dynamic light scattering (DLS, Brookhaven Ins. Corp. 90 plus particle size analyzer) with a 35 mW solid-state laser detector at an operating wavelength of 658 nm. The purity of p(NR) particles was assessed by using HPLC (Thermo Ultimate 3000) with a diode-array detector and Inertsil ODS-3 5 μm, 4.6 mm × 150 mm C18 column (GL Sciences Inc.). Briefly, NR and p(NR) particles were placed in 10 mL of methanol at 1 mg/mL concentration at room temperature at 300 rpm mixing rate for 1 h. Then, these solutions were filtered through an 0.45 μm syringe filter and analyzed with HPLC at 1 mL/min flow rate with 15 min run time at 40 °C column temperature employing 20 μL of injection volumes. The mobile phase was 230:768:2 mL acetonitrile/water/formic acid, in accordance with the literature.[22]

The structural characterizations of NR and p(NR) particles included solid-state NMR spectroscopy and FT-IR spectroscopy. NMR experiments employed a CP/MAS ^{13}C NMR method (JEOL ECZ500R, 11.75 T) at 6 kHz spinning rate. FT-IR spectroscopy was performed using a Nicolet iS10 (Thermo) in the spectral range of 4000−650 cm^{-1} at a resolution of 4 cm^{-1} using an ATR technique. TGA provided information about the thermal degradation behavior of particles and monomers. Samples weighing about 4 mg were placed in the TGA pan of the thermal analyzer (Seiko, SII TG/DTA 6300 model) and heated from 50 to 800 °C under N_2 atmosphere with 100 mL/min flow rate and a 10 °C/min heating rate, and the weight loss versus temperature was recorded. The surface charge of the phenolic particles was measured by zeta potential measurements in 0.001 M KCl using a zeta potential analyzer (Brookhaven Inst. Corp.).

Hydrolytic degradation of the particles was studied at different pHs, for example, pH 5.4 in 0.1 M citrate buffer, pH 7.4 in PBS, and pH 9 in 0.01 M borate buffer. In these experiments, p(NR) particles weighing 0.010 g were suspended in 1 mL of the buffer solutions and transferred to a dialysis membrane (molecular weight cutoff 12 000 Da, Aldrich).

DOI: 10.1021/acsomega.8b02292
ACS Omega 2018, 3, 17359−17367

Then, the dialysis membrane was placed into a closed beaker containing 30 mL of buffer solution in a shaking water bath at 37.5 °C. Hydrolytic degradation of p(NR) was determined using UV/vis spectroscopy (T80 UV/vis spectrometer, PG Ins. Ltd.) by measuring absorbance values from the elution solutions at 283 nm. The amounts of NR in the solution outside of the dialysis tubing were determined from previously constructed calibration curves at 283 nm in pH 5.4, pH 7.4, and pH 9 buffers. All experiments were carried out in triplicate, and the results are reported as the average values with standard deviation.

Antioxidant Properties of the Particles. Total phenol content of the monomers and the particle forms were evaluated by FC test according to the literature with some modifications.[23,24] For this purpose, 0.1 mL of a 170 μg/mL particle suspension was reacted with 1.25 mL of 0.2 N solution of FC phenol reagent for 4 min. Then, 1 mL of 0.7 M sodium bicarbonate solution was placed into the reaction medium and kept in the dark. After 2 h, the total phenol content or antioxidant capacity of the particles was measured by using a UV/vis spectrophotometer at 760 nm wavelength and expressed as μg/mL of gallic acid equivalents.

The antioxidant capacity of the phenolic monomers and their particle forms was also evaluated by the ABTS scavenging assay in accord with the literature with slight modification.[20,24] A solution was prepared by mixing 2.45 mM potassium persulfate (2.5 mL) and 7 mM ABTS solution in deionized (DI) water (7.5 mL); the mixture was kept in the dark for 12−16 h at 4 °C to obtain stock $ABTS^{\bullet+}$ solution. This stock $ABTS^{\bullet+}$ solution was diluted with PBS to adjust to an absorbance of 0.7 ± 0.05 at 734 nm using a UV/vis spectrophotometer. Then, 10 mL of 170 μg/mL concentration of the phenolic monomer and/or the corresponding particle suspension was prepared, and various amounts of this suspension (5−300 μL) were reacted with 3000 μL of $ABTS^{\bullet+}$ solution for 6 min. The absorbance of the diluted $ABTS^{\bullet+}$ solution without the antioxidant material at the zero time (A_{blank}) and the absorbance of the ABTS solution with antioxidant materials after 6 min reaction were recorded. The antioxidant scavenging capacity of the material was calculated using following eq 1

$$(\text{Inhibition},\ \%) = [(A_{blank} - A_{sample})/A_{blank}] \times 100 \quad (1)$$

The amount of antioxidant materials was determined for the values of 20−80% reduction of the blank absorbance. Trolox equivalent antioxidant capacity (TEAC) was determined against the slope of a trolox standard curves and expressed as "mM trolox/g of the sample".

Biocompatibility Test. Biocompatibility was assessed by a modification of a previously described method;[25] the assay described herein used 24-well rather than 12-well culture plates. After dry sterilization by UV irradiation for 2 min, p(NR) particles (1000 μg/mL) were suspended in the sterile DMEM medium that lacked labile components (glutamine, pyruvate, AA, and FBS). After 24 h at 37 °C in a 5% CO_2/95% air atmosphere, no residue of the particles was observed. This eluate was subsequently diluted with additional incomplete DMEM to generate lower concentrations of the test samples. Before use in the biocompatibility assay, these solutions were supplemented with 1/5 volume of DMEM containing 20 mM glutamine, 5 mM pyruvate, 1/20 dilution of AA, and 50% FBS. Purified monomeric NR was treated in an identical manner.

COS-1 cells from the stock culture were seeded in 24-well microassay plates at a density of 5×10^3 cells/well in 0.5 mL of complete culture medium (DMEM + 4 mM glutamine, 1 mM pyruvate, 1/100 dilution of AA, and 10% FBS). The cells were allowed to incubate in the wells at 37 °C until they attached (∼1 h); then, 1.25 mL of the supplemented culture medium containing either NR or the eluate from the NR particles was added to each well, so that each well contained a total of 1.75 mL of complete medium ± the test sample. The final concentrations of the test samples in the wells were 571, 171, 57, 17, and 0 μg/mL.

The cells were incubated at 37 °C in a 5% CO_2/95% air atmosphere for 5 days without a medium change. The culture medium was carefully removed, and the cells were washed gently three times with PBS. An aliquot (0.5 mL) of neutral buffered formalin was added to each well, and the cells were fixed for 30 min. The neutral buffered formalin was removed by aspiration and replaced with 0.5 mL of toluidine blue in neutral buffered formalin (2.5% w/v toluidine blue). After an additional 1 h incubation, the toluidine blue was removed and all of the wells were washed four times with DI water and allowed to dry for 24 h. The plates were photographed, and the cell number was subsequently assessed by solubilizing the bound toluidine blue dye in 0.5 mL of 2% sodium dodecyl sulfate/water. After 15 min, a 200 μL aliquot of the solubilized dye could be read directly at 650 nm in a 96-well plate. Strongly colored samples were diluted with water to ensure that their absorbance values were within the linear range of the microplate reader (VersaMax tunable microplate reader, Molecular Devices). For statistics, t tests were used to determine whether the viability of cells grown in the presence of NR or p(NR) particles was significantly different from the control. The data are expressed as $^*p < 0.05$, $^{**}p < 0.0001$ versus control. In a separate series of experiments, COS-1 cells were treated with NR at concentrations of 100, 300, and 1000 μg/mL as described above for phase contrast microscopy. A Nikon Eclipse TE300 phase contrast microscope equipped with an Olympus DP70 camera was used to prepare micrographs.

Blood Compatibility of NR and p(NR) Particles. The blood compatibility tests of NR and p(NR) particles were performed according to the previous studies[26,27] using a procedure approved by Human Research Ethics Committee of Canakkale Onsekiz Mart University (KAEK-2016-27).

Hemolysis Test. Fresh human blood was taken from healthy donors and immediately put into hemogram tubes containing ethylenediaminetetraacetic acid (EDTA) as the anticoagulant. Separately, a concentrated stock of NR or p(NR) particles was prepared at 10 mg/mL in 0.9% saline solution. This stock was further diluted by suspending 0, 25, 50, and 100 μL of the stock into 10 mL of 0.9% saline solution at 37.5 °C. Then, 2 mL of blood was diluted with 2.5 mL of 0.9% saline solution at 37.5 °C, and 0.2 mL of this diluted blood was added into NR and p(NR) particle suspensions. These samples were incubated in a shaking bath at 37.5 °C for 1 h and then centrifuged at 100g for 5 min. The absorbance of each supernatant was measured at 542 nm to quantify the amount of hemolysis (A_{sample}). The absorbance of 0.2 mL of diluted blood in 10 mL of water was used as a positive control ($A_{positive}$), and the absorbance of 0.2 mL of diluted blood in 10 mL of saline solution was used as a negative control ($A_{negative}$). The hemolysis ratio of the materials was calculated by following eq 2

DOI: 10.1021/acsomega.8b02292
ACS Omega 2018, 3, 17359−17367

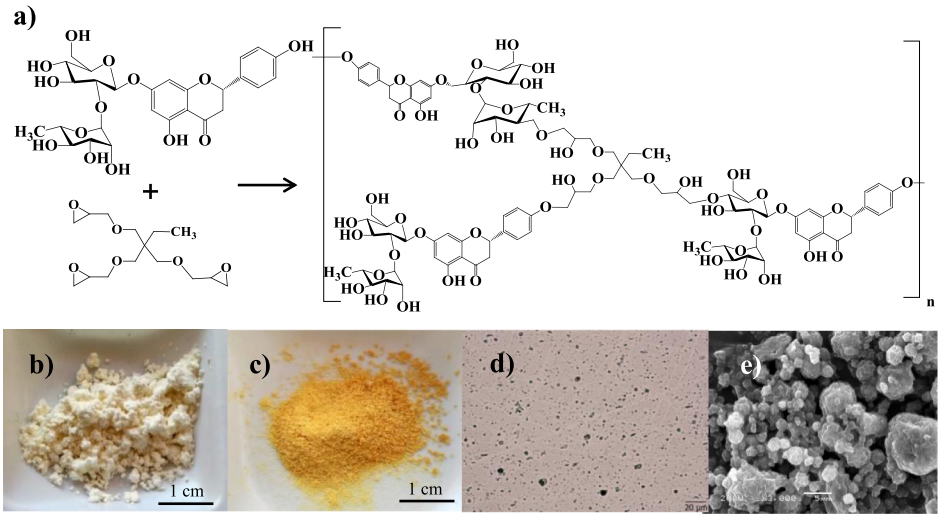

Figure 1. (a) Schematic representation of the polymerization of p(NR) particles from NR; (b) NR powder; (c) dried p(NR) particles; (d) light microscopy of p(NR); and (e) SEM image of p(NR) particles.

$$\text{Hemolysis ratio \%} = (A_{\text{sample}} - A_{\text{negative}})/(A_{\text{positive}} - A_{\text{negative}}) \times 100 \quad (2)$$

The analysis was repeated three−six times, and the average values with standard deviations are reported.

Blood Clotting Test. Fresh human blood was taken from healthy donors and immediately put into hemogram tubes containing EDTA as the anticoagulant. Separately, a 10 mg/mL suspension of NR and p(NR) particles was dispersed in 0.9% saline solution and four different amounts: 10, 25, 50, 100 μL were placed into flat-bottomed centrifuge tubes. Then, 0.24 mL of 0.2 M $CaCl_2$ solution was added to 3 mL of blood, and 0.27 mL of this blood−$CaCl_2$ mixture was layered on top of the NR-based materials and incubated at 37.5 °C in a shaking bath. After 10 min, 10 mL of DI water was added to each tube and the tubes were subsequently centrifuged at 100*g* for 30 s to pellet the clot. The supernatant solution, containing free red blood cells, was removed, diluted with 40 mL of DI, and incubated at 37.5 °C with shaking for 1 h. The absorbance of the blood sample in contact with NR or p(NR) (A_{sample}) and the absorbance of the diluted blood (0.25 mL of blood in 50 mL of DI water) (A_{blood}) were measured by using a UV/vis spectrophotometer at 542 nm. Blood clotting index of the materials was calculated by following eq 3

$$\text{Blood clotting index} = (A_{\text{particle+blood}}/A_{\text{blood}}) \times 100 \quad (3)$$

The analysis was repeated three to six times, and the means with standard deviations are reported.

***α*-Glucosidase Activity Assays.** NR and p(NR) particles were dissolved or suspended in 67 mM pH 6.9 phosphate buffer solution at a concentration of 5 mg/mL and incubated at 37.5 °C in a shaking bath for 24 h. The solutions were subsequently filtered through an 0.22 μm pore size filter and diluted to different concentrations (0.5, 1.0, 2.0, 4.0, and 5.0 mg/mL) with 67 mM pH 6.9 phosphate buffer.

The α-glucosidase assays were performed using the colorimetric substrate, *p*-nitrophenyl-α-D-glucopyranoside, according to the technical information provided by the manufacturer. Briefly, sample solutions (70 μL) with different concentrations of monomer or eluate from dissolved particles (0.5, 1.0, 2.0, 4.0, and 5.0 mg/mL) were mixed with α-glucosidase solution (70 μL, 0.02 U/mL in 67 mM phosphate buffer, pH 6.9 containing 0.2 mM reduced glutathione). The mixtures were incubated in 96-well plates at 25 °C for 10 min. The substrate (70 μL of 5 mM *p*-nitrophenyl-α-D-glucoside solution in 67 mM phosphate buffer, pH 6.9) was then added to each well at timed intervals. The reaction mixtures were incubated at 25 °C for 15 min. Before and after incubation, the absorbance readings were recorded at 405 nm using a VersaMax tunable microplate reader (Molecular Devices) and compared to a control which had 70 μL of buffer solution in place of the NR or p(NR) eluate.

The effect of NR or p(NR) particles on α-glucosidase activity was calculated as the fraction of activity, as compared to the sample without added NR monomer or p(NR) eluate, using eq 4

$$\text{Fraction of activity} = \frac{\text{Abs}_{405}^{\text{sample}}}{\text{Abs}_{405}^{\text{control}}} \quad (4)$$

where $\text{Abs}_{405}^{\text{control}}$ is the color (absorbance at 405 nm) developed in the absence of added NR monomer or particle eluate and $\text{Abs}_{405}^{\text{sample}}$ is the color (absorbance at 405 nm) developed in the presence of the added NR monomer or p(NR) eluate.

RESULTS AND DISCUSSION

In the preparation of p(NR) particles, a water-in-oil microemulsion cross-linking method was used. As illustrated in Figure 1, the NR particles are formed readily within the water phase of the lecithin/gasoline system, via cross-linking of hydroxyl groups on the NR unit with TMPGDE. It is apparent from the SEM images that p(NR) particles are within the size range of 1−10 μm.

The purity of the p(NR) particles was tested using HPLC and compared with the NR monomer; the corresponding chromatograms are provided as Figure S1 (in the Supporting Information). In the NR chromatogram, obtained from 1 mg/mL NR in methanol solution, there is a solvent peak that elutes between 1.4 and 2.4 min and a peak for NR at 6.25 min. Similarly, the chromatogram of p(NR) particles revealed the same peaks because of the degradation of p(NR) into the monomer. The absence of additional peaks in the HPLC

DOI: 10.1021/acsomega.8b02292
ACS Omega 2018, 3, 17359−17367

analyses confirms that there are no significant contaminants in the synthesized p(NR) particles.

The structural analysis of NR and p(NR) particles was performed using solid-state NMR employing proton decoupled ^{13}C NMR spectroscopy, and corresponding result is shown in the Supporting Information as Figure S2a,b. All of the chemical shifts for NR were assigned in according to the literature,[28] and we discovered that there were some chemical shifts upon p(NR) particle formation. In the ^{13}C NMR spectra of p(NR) particles, some characteristic changes in the C atom shifts occurred when compared with the spectrum of the NR. The C═O(7) carbon, observed at δ = 245 ppm for NR, is shifted to δ = 247 ppm for the p(NR) particle. The aromatic carbon signals of particles C1 to C6 and C10 to C13 were observed at 104−213 ppm regions, as shown in Supporting Information Figure S2b. The saccharide carbons of p(NR) chemical shifts are greater than those of the NR monomer; they are appeared between δ = 66−100 ppm for p(NR) particles in comparison to δ = 65−94 ppm for the NR monomer. Surprisingly, the chemical shifts for $-CH_3$(25) and $-CH_2$(8) carbons were observed in the high region with 23 and 41 ppm chemical shifts, respectively, whereas the chemical shift for CH_2OH(19) carbon was observed in the low chemical region with 45 ppm chemical shift for p(NR) particles.

FT-IR spectroscopy was used for functional group analysis and structural characterization of phenolic particles. For this purpose, the FT-IR spectrum of the phenolic monomer, NR, and its corresponding polymeric particles was recorded, as shown in Figure 2a. Because all of the phenolic monomers used in this study possess −OH groups attached to the benzene rings and NR also has −OH groups from glycoside structure, a clear wide peak between 3000 and 3500 cm^{-1} can be assigned to −OH stretching.

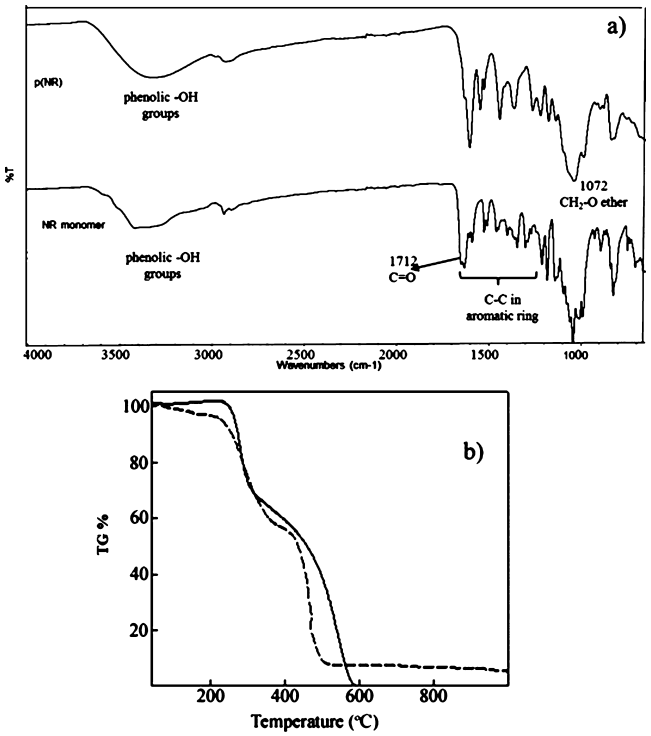

Figure 2. (a) FT-IR spectra of NR and p(NR) particles. (b) Thermogram of NR (solid line) and p(NR) particles (dashed line).

Also, the common bonds such as carbonyl (C═O) and C−C for benzene rings were all observed in the 1680−1750 range, and at about 1500−1700 cm^{-1} range in accordance with IR atlas.[23,29] Upon cross-linking of all of the phenolic monomers with the epoxide-based cross-linker, the new ether bonds formed as a result of the cross-linking are shown with stretching frequencies of about 1072 and 1077 cm^{-1} for all p(NR) particles, as given in Figure 2a. Furthermore, the intensity of the −OH stretching frequency between 3000 and 3500 cm^{-1} belonging to −OH groups is increased because of cross-linking of NR units with TMPGDE.

For thermal characterization, TGA of NR and p(NR) is shown in Figure 2b. According to the thermogram, NR was degraded at two steps from 243 to 319 °C with 31.4% weight loss in the first step; the main degradation started at 354 °C, and NR was totally degraded at 589 °C. For the p(NR) particles, the slight weight loss (4%) observed between 74 and 211 °C was most likely related to bound water and then two main degradations were observed at 224−513 and 412−513 °C with a 38.3 and 53.7% weight loss, respectively. Finally, 5.1% residual material was determined at 994 °C for p(NR) particles, most likely because of the cross-linker in the polymer structure.

To assess the surface charge characteristic of the prepared p(NR) particles, zeta potential measurements at different pH conditions were performed in 0.001 M KCl solution and results are summarized in Figure 3. It is obvious that as the pH

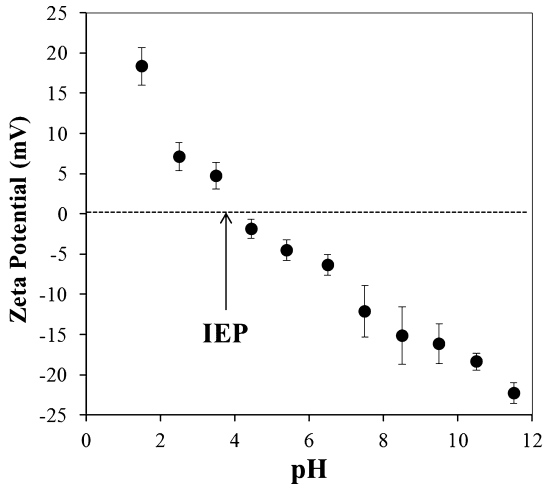

Figure 3. Zeta potential values of p(NR) particles at different pH conditions in 0.001 M KCl solution. The IEP (4.0) is indicated by the arrow. Data represent mean ± standard deviation (SD) (n = 3).

of the solution increases, the zeta potential values of the particles decrease because of the acidic character of the NR. The isoelectric point (IEP), as determined from zeta potential measurements at various pHs, was at pH 4.0, as indicated by the arrow. Additionally, the size of particles was measured with DLS after filtration of the particle suspension with a 2 μm filter. The size of p(NR) was in the 535 nm range (primary data not shown) and thus at the lower end of the size range determined via SEM analysis.

To determine the degradation profile of p(NR) in different pH media, a small quantity of the particles (10 mg/mL) was suspended in suitable buffer solutions, transferred to dialysis membranes, and placed in buffers with the pH values of 5.4, 7.4, and 9. The amount of NR released from the particles was

DOI: 10.1021/acsomega.8b02292
ACS Omega 2018, 3, 17359−17367

measured by UV/vis spectroscopy of the surrounding solution, using previously prepared calibration curves of NR, as described in the Experimental Section. Figure 4 shows the degradation profile of p(NR) particles in different pH buffers.

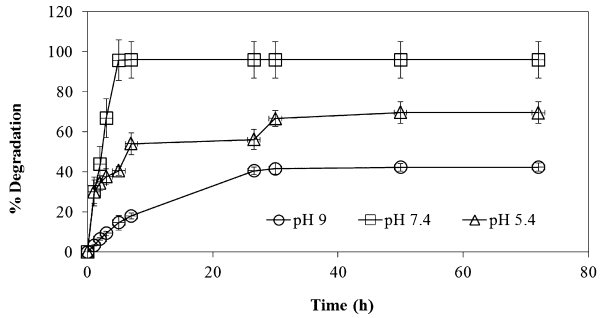

Figure 4. Degradation of p(NR) particles at pHs 5.4, 7.4, and 9. Data represent mean ± SD (n = 3).

As can be seen from Figure 4, physiological pH (7.4) is the most effective pH for p(NR) particle degradation; 95 ± 8.9% of p(NR) is degraded in about 5 h. The lowest rate of degradation was observed at pH 9 where 42 ± 1.2% degradation was observed. At pH 5.4, 69 ± 5.3% degradation was seen at the end of the third day, with no additional degradation at longer incubation times.

The antioxidant activity of NR and p(NR) was assessed using both total phenol content and TEAC, with gallic acid as the reference compound, and the results are summarized in Table 1.

Table 1. Total Phenol Content and TEAC Values of NR and p(NR)

antioxidant materials	total phenol content, as gallic acid equivalents[a] (μg/mL)	TEAC values (μmol trolox equivalents/g)
NR	2.74 ± 0.8	0.26 ± 0.02
NR particles	2.78 ± 0.4	0.25 ± 0.02
gallic acid	170.0 ± 0.00	9.14 ± 0.43

[a]NR, p(NR) and gallic acid were assessed at concentrations of 170 μg/mL.

As can be seen in Table 1, NR and p(NR) had very modest antioxidant activity when compared to gallic acid, one of the most widely used standard materials for antioxidant properties. The total phenol content of NR and p(NR) particles was 2.74 and 2.78 μg/mL, respectively, as compared to gallic acid, whose phenol content was more than 60-fold higher (170 μg/mL). A second measure of antioxidant capacity, TEAC, also showed that NR and p(NR) were ∼36 times less active than gallic acid, 0.26 and 0.25 μmol trolox equivalent/g, respectively, compared to 9.14/g for gallic acid. These results are in agreement with other studies, which have also reported low antioxidant activity of NR in both in vivo and in vitro studies.[30−32] The disaccharide present in NR may contribute to its low antioxidant activity; previous studies have reported that the sugar moieties cause steric hindrance of the scavenging group.[33]

Tests for biocompatibility of the phenolic molecules and the corresponding particles were carried out using the COS-1 cell line. Figure 5 illustrates the biocompatibility of NR and p(NR), expressed as % viability as compared to cells grown for 5 days without added NR or p(NR). Both the monomer and the polymerized particles showed very good biocompatibility. Only at the highest concentration tested (571 μg/mL) was any cytotoxicity detected and even these levels had a minimal effect; viability was 96.7 ± 0.93% for NR and 91 ± 11% or p(NR).

In a separate series of experiments, COS-1 cells were treated with varying concentrations of NR monomer and cell morphology was assessed by phase contract microscopy (Figure S3 in the Supporting Information). NR concentrations of 100 and 300 μg/mL had no statistically significant effect on cell morphology (Figure S3, panels b,c, respectively) or cell number. However, at a concentration of 1000 μg/mL (panel d), the NR was not completely soluble and the NR crystals present on the cell cultures reduced the cell by ∼75% (primary data not shown). Thus, the solubility of NR may ultimately control its cell toxicity. A similar lack of NR toxicity has been reported for nucleus pulposus cells and mesenchymal stem cells.[34,35] The low level of toxicity may have been due to the presence of the disaccharide moiety in NR. Koganov et al. have reported that quercetin (a polyphenol) was a strong fibroblast growth inhibitor, whereas its corresponding glycoside, rutin, did not possess this toxicity.[36]

It is important to note that the effects of NR may differ for different cell types. Glioblastomas are the most aggressive cancer of the brain. NR exhibits inhibitory effects on the invasion and adhesion of U87, a human glioblastoma cell line. NR inhibited cell invasion into Matrigel in a concentration-dependent manner and also inhibited the migration of U87 cells in a concentration-dependent manner in a wound-healing assay.[37]

NR and p(NR) particles were also tested for their blood compatibility, and the results are shown in Figure 6.

Hemolysis is the rupture of red blood cells with the release of their contents, and the maximum hemolysis ratio must be under 5% for biocompatible materials.[26] Hemolysis was significantly greater than controls with no added NR or p(NR) ($p < 0.0001$) for all concentrations tested, but NR and p(NR) both showed acceptable properties. In general, the p(NR) particles appeared to induce less hemolysis than corresponding levels of NR, as shown in Figure 6a. The effect of p(NR) on blood clotting is shown in Figure 6b, with data reported as the blood clotting index. An index of 100 indicates no effect, an index >100 indicates that the biomaterial interferes with blood clotting, whereas an index <100 indicates that the material under study stimulates clotting.[26] The data show that p(NR) has a minor stimulatory effect on blood clotting at all concentrations tested, whereas NR has much less effect at the same concentrations.[38] Thus, NR is safe for blood with the minimum 80.6 ± 1.2% blood clotting index up to 100 μg/mL. p(NR) has a slightly little lower compatibility, with the minimum 73.08 ± 2.1% blood clothing index up to 50 μg/mL. The highest concentration of p(NR) tested (100 μg/mL) has a blood clotting index of 51.9 ± 13.7.

As a final test of biocompatibility, the effect NR and p(NR) on α-glucosidase activity was determined. The enzyme α-glucosidase is very important for carbohydrate absorption in the small intestine, and many natural products have been reported to inhibit the degradation of maltose to glucose, the final step before the entry of glucose into the bloodstream.[39,40] It is now believed that inhibition of the enzymes involved in the digestion of carbohydrates can significantly decrease the postprandial increase of blood glucose level after a mixed

DOI: 10.1021/acsomega.8b02292
ACS Omega 2018, 3, 17359−17367

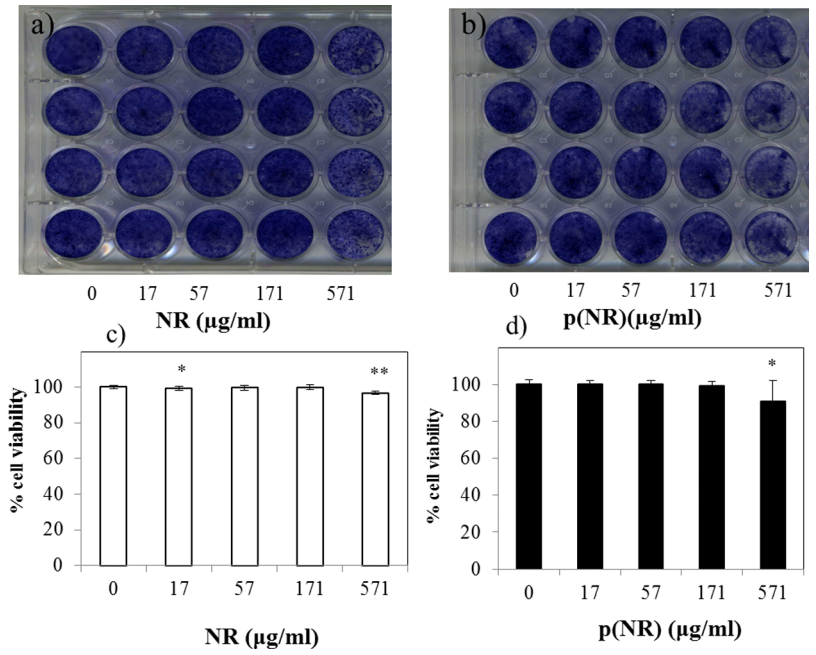

Figure 5. Representative photographs of 24-well cell culture plate after fixation and toluidine blue staining. (a) Treatment with NR and (b) treatment with NR particles p(NR). Cell-bound dye was eluted from the plates and quantified as absorbance at 650 nm. Cell viability was expressed as the % color in control cultures. (c) Treatment with NR monomer (NR) or (d) NR particles p(NR). Data represent mean ± SD (n = 3). A t-test was used to determine if treated samples were significantly different from the control; *p < 0.05, **p < 0.0001 vs control.

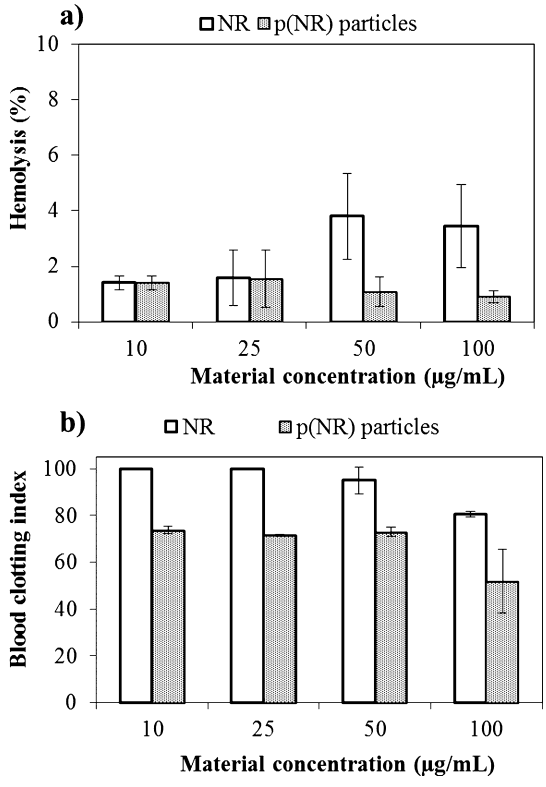

Figure 6. (a) Hemolysis (%) induced by NR and p(NR) particles at different concentrations. (b) Blood clotting index of p(NR) at different concentrations. Data represent mean ± SD (n = 3).

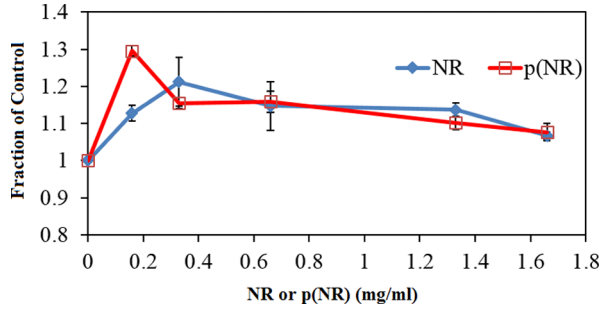

Figure 7. Effect of NR and p(NR) on α-glucosidase activity. Data are reported as a fraction of activity in the absence of NR or p(NR) particles at the indicated concentrations.

carbohydrate diet and therefore can be an important strategy in the management of type-II diabetes.[41] As shown in Figure 7, low levels (0.17 mg/mL) of NR and p(NR) stimulated α-glucosidase by 13 and 30%, respectively. At higher concentrations of NR and p(NR) (0.33−1.67 mg/mL), the stimulatory activity decreased in a dose-dependent fashion, from 20 to 7%, but there were no significant differences between NR and p(NR) at these concentrations.

Literature on the properties of herbal extracts suggests that there is a strong correlation between antioxidant activity and the inhibition of enzymes involved in carbohydrate digestion.[40] In the present studies, there is a similar correlation between the modest antioxidant activity of NR and p(NR) particles and the failure of these agents to inhibit α-glucosidase. In our experiments, NR and p(NR) have low antioxidant properties and actually stimulate α-glucosidase activity, as assessed with a colorimetric substrate.

CONCLUSIONS

Polyphenolic particles of cross-linked NR can be prepared in an oil-in-water microemulsion system in a single step using TMPGDE as a cross-linker. These particles possess negative surface charges, suggesting the abundant amounts of −OH functionality that can be further used for drug conjugation

DOI: 10.1021/acsomega.8b02292
ACS Omega 2018, 3, 17359−17367

and/or other biomedical applications. Synthesized p(NR) particles are biodegradable at physiological pH and have high biocompatibility, blood compatibility, and low antioxidant properties. In general, polyphenols show α-glucosidase inhibitory activity; however, NR and its corresponding particles do not inhibit α-glucosidase and even show a modest ability to stimulate this activity enzyme (~7−30%), depending upon the concentration.

Now that biocompatibility has been established, future studies will concentrate upon developing p(NR) particles as an adjunct to drug delivery that can enhance the pharmacokinetic properties of specific drug classes. NR is rapidly converted to its aglycone, naringenin, by bacterial in the small intestine,[42] and naringenin is a known inhibitor of the Pgp transporter in intestinal epithelial cells.[43] Because of the Pgp transporter's localization on the side of the epithelial cell membrane that faces the gut lumen, this transporter pumps many orally administered drugs back into the lumen and thus inhibits their absorption.[44] Both in vitro and in vivo studies have demonstrated that inhibition of this transporter significantly increases drug absorption.[45−47] Recent in vivo studies with NR have shown that its co-administration with both tamoxifen and colchicine enhances drug bioavailability.[48,49] The slow, controlled release of NR, from the p(NR) particles described herein, as they transit through the gut lumen, could provide a unique new tool for drug delivery.

■ ASSOCIATED CONTENT

Supporting Information

The Supporting Information is available free of charge on the ACS Publications website at DOI: 10.1021/acsomega.8b02292.

HPLC chromatographs of NR and p(NR) particles; NMR of NR and p(NR) particles; and phase contrast micrographs of COS-1 cells treated with NR (PDF)

■ AUTHOR INFORMATION

Corresponding Authors

*E-mail: sahiner71@gmail.com (N.S.).
*E-mail: blake@tulane.edu (D.A.B.).

ORCID

Mehtap Sahiner: 0000-0001-8666-7954
Nurettin Sahiner: 0000-0003-0120-530X
Mitchell L. Fullerton: 0000-0003-2285-558X
Diane A. Blake: 0000-0002-7532-1541

Notes

The authors declare no competing financial interest.

■ ACKNOWLEDGMENTS

M.S. was supported by the Scientific and Technological Research Council of Turkey (TUBITAK) BİDEB-2219 Postdoctoral Research program grant number 1059B191600622. Additional research funds were provided by a Research Enhancement Grant from Tulane University School of Medicine to D.A.B.

■ REFERENCES

(1) Tripoli, E.; La Guardia, M.; Giammanco, S.; Di Majo, D.; Giammanco, M. Citrus flavonoids: Molecular structure, biological activity and nutritional properties: A review. *Food Chem.* **2007**, *104*, 466−479.

(2) You, H. J.; Ahn, H. J.; Ji, G. E. Transformation of Rutin to Antiproliferative Quercetin-3-glucoside byAspergillus niger. *J. Agric. Food Chem.* **2010**, *58*, 10886−10892.

(3) Lee, S. J.; Kim, J.-C.; Kim, M. J.; Kitaoka, M.; Park, C. S.; Lee, S. Y.; Ra, M.-J.; Moon, T. W.; Robyt, J. F.; Park, K. H. Trans-glycosylation of Naringin byBacillusstearothermophilusMaltogenic Amylase To Give Glycosylated Naringin. *J. Agric. Food Chem.* **1999**, *47*, 3669−3674.

(4) Lv, J.; Sun, X.; Ma, J.; Ma, X.; Xing, G.; Wang, Y.; Sun, L.; Wang, J.; Li, F.; Li, Y. Involvement of periostin-sclerostin-Wnt/β-catenin signaling pathway in the prevention of neurectomy-induced bone loss by naringin. *Biochem. Biophys. Res. Commun.* **2015**, *468*, 587−593.

(5) Ramakrishnan, A.; Vijayakumar, N. Urea cycle pathway targeted therapeutic action of naringin against ammonium chloride induced hyperammonemic rats. *Biomed. Pharmacother.* **2017**, *94*, 1028−1037.

(6) Ahmed, O. M.; Hassan, M. A.; Abdel-Twab, S. M.; Abdel Azeem, M. N. Navel orange peel hydroethanolic extract, naringin and naringenin have anti-diabetic potentials in type 2 diabetic rats. *Biomed. Pharmacother.* **2017**, *94*, 197−205.

(7) Ji, Y.; Wang, L.; Watts, D. C.; Qiu, H.; You, T.; Deng, F.; Wu, X. Controlled-release naringin nanoscaffold for osteoporotic bone healing. *Dent. Mater.* **2014**, *30*, 1263−1273.

(8) Gorinstein, S.; Leontowicz, H.; Leontowicz, M.; Krzeminski, R.; Gralak, M.; Delgado-Licon, E.; Martinez Ayala, A. L.; Katrich, E.; Trakhtenberg, S. Changes in plasma lipid and antioxidant activity in rats as a result of naringin and red grapefruit supplementation. *J. Agric. Food Chem.* **2005**, *53*, 3223−3228.

(9) Hu, Y.; Li, Y.; Zhang, W.; Kou, G.; Zhou, Z. Physical stability and antioxidant activity of citrus flavonoids in arabic gum-stabilized microcapsules: Modulation of whey protein concentrate. *Food Hydrocolloids* **2018**, *77*, 588−597.

(10) Kola, P. K.; Akula, A.; NissankaraRao, L. S.; Sekhara Reddy Danduga, R. C. Protective effect of naringin on pentylenetetrazole (PTZ)-induced kindling; possible mechanisms of antikindling, memory improvement, and neuroprotection. *Epilepsy Behav.* **2017**, *75*, 114−126.

(11) Qin, S.; Chen, Q.; Wu, H.; Liu, C.; Hu, J.; Zhang, D.; Xu, C. Effects of naringin on learning and memory dysfunction induced by gp120 in rats. *Brain Res. Bull.* **2016**, *124*, 164−171.

(12) Rao, K.; Imran, M.; Jabri, T.; Ali, I.; Perveen, S.; Shafiullah; Ahmed, S.; Shah, M. R. Gum tragacanth stabilized green gold nanoparticles as cargos for Naringin loading: A morphological investigation through AFM. *Carbohydr. Polym.* **2017**, *174*, 243−252.

(13) Viswanatha, G. L.; Shylaja, H.; Moolemath, Y. The beneficial role of Naringin- a citrus bioflavonoid, against oxidative stress-induced neurobehavioral disorders and cognitive dysfunction in rodents: A systematic review and meta-analysis. *Biomed. Pharmacother.* **2017**, *94*, 909−929.

(14) Xianchu, L.; Lan, Z.; Qiufang, L.; Yi, L.; Xiangcheng, R.; Wenqi, H.; Yang, D. Naringin protects against lipopolysaccharide-induced cardiac injury in mice. *Environ. Toxicol. Pharmacol.* **2016**, *48*, 1−6.

(15) Zhang, L.; Song, L.; Zhang, P.; Liu, T.; Zhou, L.; Yang, G.; Lin, R.; Zhang, J. Solubilities of Naringin and Naringenin in Different Solvents and Dissociation Constants of Naringenin. *J. Chem. Eng. Data* **2015**, *60*, 932−940.

(16) Ren, X.; Shi, Y.; Zhao, D.; Xu, M.; Li, X.; Dang, Y.; Ye, X. Naringin protects ultraviolet B-induced skin damage by regulating p38 MAPK signal pathway. *J. Dermatol. Sci.* **2016**, *82*, 106−114.

(17) Yu, M.; You, D.; Zhuang, J.; Lin, S.; Dong, L.; Weng, S.; Zhang, B.; Cheng, K.; Weng, W.; Wang, H. Controlled Release of Naringin in Metal-Organic Framework-Loaded Mineralized Collagen Coating to Simultaneously Enhance Osseointegration and Antibacterial Activity. *ACS Appl. Mater. Interfaces* **2017**, *9*, 19698−19705.

(18) Fuhr, U. Drug Interactions with Grapefruit Juice. *Drug Saf.* **1998**, *18*, 251−272.

(19) Bailey, D. G.; Dresser, G. K.; Leake, B. F.; Kim, R. B. Naringin is a major and selective clinical inhibitor of organic anion-transporting

DOI: 10.1021/acsomega.8b02292
ACS Omega 2018, 3, 17359−17367

polypeptide 1A2 (OATP1A2) in grapefruit juice. *Clin. Pharmacol. Ther.* **2007**, *81*, 495−502.
(20) Shirasaka, Y.; Suzuki, K.; Nakanishi, T.; Tamai, I. Differential effect of grapefruit juice on intestinal absorption of statins due to inhibition of organic anion transporting polypeptide and/or P-glycoprotein. *J. Pharm. Sci.* **2011**, *100*, 3843−3853.
(21) Kamel, A.; Harriman, S. Inhibition of cytochrome P450 enzymes and biochemical aspects of mechanism-based inactivation (MBI). *Drug Discovery Today: Technol.* **2013**, *10*, e177−e189.
(22) Büyüktuncel, E. Fast determination of naringin and hesperidin in natural and commercial citrus juices by HPLC method. *Asian J. Chem.* **2017**, *29*, 2384−2386.
(23) Sahiner, N.; Sagbas, S.; Aktas, N.; Silan, C. Inherently antioxidant and antimicrobial tannic acid release from poly(tannic acid) nanoparticles with controllable degradability. *Colloids Surf., B* **2016**, *142*, 334−343.
(24) Sahiner, M.; Sagbas, S.; Bitlisli, B. O. p(AAm/TA)-based IPN hydrogel films with antimicrobial and antioxidant properties for biomedical applications. *J. Appl. Polym. Sci.* **2015**, *132*, 41876.
(25) Ponnusamy, T.; Yu, H.; John, V. T.; Ayyala, R. S.; Blake, D. A. A Novel Antiproliferative Drug Coating for Glaucoma Drainage Devices. *J. Glaucoma* **2014**, *23*, 526−534.
(26) Shih, M.-F.; Shau, M.-D.; Chang, M.-Y.; Chiou, S.-K.; Chang, J.-K.; Cherng, J.-Y. Platelet adsorption and hemolytic properties of liquid crystal/composite polymers. *Int. J. Pharm.* **2006**, *327*, 117−125.
(27) Sahiner, N.; Sagbas, S. Sucrose based ionic liquid colloidal microgels in separation of biomacromolecules. *Sep. Purif. Technol.* **2018**, *196*, 191−199.
(28) Tsujimoto, T.; Yoshitomi, T.; Maruyama, T.; Yamamoto, Y.; Hakamatsuka, T.; Uchiyama, N. 13C-NMR-based metabolic fingerprinting of Citrus-type crude drugs. *J. Pharm. Biomed. Anal.* **2018**, *161*, 305−312.
(29) Sahiner, N.; Sagbas, S.; Aktas, N. Single step natural poly(tannic acid) particle preparation as multitalented biomaterial. *Mater. Sci. Eng., C* **2015**, *49*, 824−834.
(30) Yu, J.; Wang, L.; Walzem, R. L.; Miller, E. G.; Pike, L. M.; Patil, B. S. Antioxidant activity of citrus limonoids, flavonoids, and coumarins. *J. Agric. Food Chem.* **2005**, *53*, 2009−2014.
(31) Andrade, J. E.; Burgess, J. R. Effect of the citrus flavanone naringenin on oxidative stress in rats. *J. Agric. Food Chem.* **2007**, *55*, 2142−2148.
(32) Bacanlı, M.; Ahmet Başaran, A.; Başaran, N. The antioxidant and antigenotoxic properties of citrus phenolics limonene and naringin. *Food Chem. Toxicol.* **2015**, *81*, 160−170.
(33) Ashraful Alam, M.; Subhan, N.; Mahbubur Rahman, M.; Uddin, S. J.; Reza, H. M.; Sarker, S. D. Effect of citrus flavonoids, naringin and naringenin, on metabolic syndrome and their mechanisms of action. *Adv. Nutr.* **2014**, *5*, 404−417.
(34) Li, N.; Whitaker, C.; Xu, Z.; Heggeness, M.; Yang, S.-Y. Therapeutic effects of naringin on degenerative human nucleus pulposus cells for discogenic low back pain. *Spine J.* **2016**, *16*, 1231−1237.
(35) Cao, X.; Lin, W.; Liang, C.; Zhang, D.; Yang, F.; Zhang, Y.; Zhang, X.; Feng, J.; Chen, C. Naringin rescued the TNF-α-induced inhibition of osteogenesis of bone marrow-derived mesenchymal stem cells by depressing the activation of NF-κB signaling pathway. *Immunol. Res.* **2015**, *62*, 357−367.
(36) Koganov, M. M.; Dueva, O. V.; Tsorin, B. L. Activities of plant-derived phenols in a fibroblast cell culture model. *J. Nat. Prod.* **1999**, *62*, 481−483.
(37) Aroui, S.; Aouey, B.; Chtourou, Y.; Meunier, A.-C.; Fetoui, H.; Kenani, A. Naringin suppresses cell metastasis and the expression of matrix metalloproteinases (MMP-2 and MMP-9) via the inhibition of ERK-P38-JNK signaling pathway in human glioblastoma. *Chem.-Biol. Interact.* **2016**, *244*, 195−203.
(38) Barba, B. J. D.; Tranquilan-Aranilla, C.; Abad, L. V. Hemostatic potential of natural/synthetic polymer based hydrogels crosslinked by gamma radiation. *Radiat. Phys. Chem.* **2016**, *118*, 111−113.
(39) Zhu, F.; Asada, T.; Sato, A.; Koi, Y.; Nishiwaki, H.; Tamura, H. Rosmarinic Acid Extract for Antioxidant, Antiallergic, and α-Glucosidase Inhibitory Activities, Isolated by Supramolecular Technique and Solvent Extraction from Perilla Leaves. *J. Agric. Food Chem.* **2014**, *62*, 885−892.
(40) McCue, P. P.; Shetty, K. Inhibitory effects of rosmarinic acid extracts on porcine pancreatic amylase in vitro. *Asia Pac. J. Clin. Nutr.* **2004**, *13*, 101−106.
(41) Kwon, Y. I.; Vattem, D. A.; Shetty, K. Evaluation of clonal herbs of Lamiaceae species for management of diabetes and hypertension. *Asia Pac. J. Clin. Nutr.* **2006**, *15*, 107−118.
(42) Kim, D.-H.; Jung, E.-A.; Sohng, I.-S.; Han, J.-A.; Kim, T.-H.; Han, M. J. Intestinal bacterial metabolism of flavonoids and its relation to some biological activities. *Arch. Pharmacal Res.* **1998**, *21*, 17−23.
(43) Romiti, N.; Tramonti, G.; Donati, A.; Chieli, E. Effects of grapefruit juice on the multidrug transporter P-glycoprotein in the human proximal tubular cell line HK-2. *Life Sci.* **2004**, *76*, 293−302.
(44) Lin, J. H.; Yamazaki, M. Role of P-Glycoprotein in Pharmacokinetics. *Clin. Pharmacokinet.* **2003**, *42*, 59−98.
(45) Weinheimer, M.; Fricker, G.; Burhenne, J.; Mylius, P.; Schubert, R. The application of P-gp inhibiting phospholipids as novel oral bioavailability enhancers - An in vitro and in vivo comparison. *Eur. J. Pharm. Sci.* **2017**, *108*, 13−22.
(46) Zhao, W.; Uehera, S.; Tanaka, K.; Tadokoro, S.; Kusamori, K.; Katsumi, H.; Sakane, T.; Yamamoto, A. Effects of Polyoxyethylene Alkyl Ethers on the Intestinal Transport and Absorption of Rhodamine 123: A P-glycoprotein Substrate by In Vitro and In Vivo Studies. *J. Pharm. Sci.* **2016**, *105*, 1526−1534.
(47) Sparreboom, A.; van Asperen, J.; Mayer, U.; Schinkel, A. H.; Smit, J. W.; Meijer, D. K. F.; Borst, P.; Nooijen, W. J.; Beijnen, J. H.; van Tellingen, O. Limited oral bioavailability and active epithelial excretion of paclitaxel (taxol) caused by P-glycoprotein in the intestine. *Proc. Natl. Acad. Sci. U.S.A.* **1997**, *94*, 2031−2035.
(48) Choi, J.-S.; Kang, K. W. Enhanced tamoxifen bioavailability after oral administration of tamoxifen in rats pretreated with naringin. *Arch. Pharmacal Res.* **2008**, *31*, 1631−1636.
(49) Dahan, A.; Amidon, G. L. Grapefruit Juice and its Constituents Augment Colchicine Intestinal Absorption: Potential Hazardous Interaction and the Role of P-Glycoprotein. *Pharm. Res.* **2008**, *26*, 883−892.

DOI: 10.1021/acsomega.8b02292
ACS Omega 2018, 3, 17359−17367